

THE SUB- AND QUASI-CENTURIAL CYCLES IN SOLAR AND GEOMAGNETIC ACTIVITY DATA SERIES

Boris Komitov¹, Stefano Sello², Peter Duchlev¹, Momchil Dechev¹, Kaloyan Penev³ and Kostadinka Koleva¹

¹ Institute of Astronomy, 72 Tsarigradsko Chaussee, Sofia 1784, Bulgaria

² Mathematical and Physical Models, Enel Research, Via Andrea Pisano 120, 56122 Pisa - Italy;

³ Harvard University, Mail Stop 10, 60 Garden Street, Cambridge, MA 02138

ABSTRACT

The subject of this paper is the existence and stability of solar cycles with duration in the range of 20–250 years. Five type of data series are used: 1) The Zurich series (1749-2009), the mean annual International sunspot number Ri ; 2) The Group sunspot number series Rh (1610-1995); 3) The simulated extended sunspot Rsi number from Extended time series of Solar Activity Indices (ESAI) (1090- 2002); 4) The simulated extended geomagnetic aa -index from ESAI (1099-2002); 5) The Meudon filament series (1919-1991) (it is used only particularly). Data series are smoothed over 11 years and supercentennial trends are removed. Two principally independent methods of time series analysis are used: the T-R periodogram analysis (both in the standard and “scanning window” regimes) and the wavelet-analysis. The obtained results are very similar. It is found that in all series a strong cycle with mean duration of 55-60 years exists. It is very well expressed in the 18th and the 19th centuries. It is less pronounced during the end of the 19th and the beginning of the 20th centuries. On the other hand a strong and stable quasi 110-120 years and ~200-year cycles are obtained in all of these series. They are good proxies for the solar corpuscular activity events (the Group sunspot number, the aa -index and the extended Ri -series). However the 200-yr cycle is not detectable in the Zurich series. There is a strong mean oscillation of ~ 95 years , which is absent in the other data sets. The analysis of the ESAI (AD 1090-2002) proved that the quasi century cycle has a relatively stable doublet (~80 and ~120 years) or triplet (~55-60, 80 and 120 years) structure during the last ~900 years. An interesting feature in all series is the existence of significant ~29-year cycle after the last centennial Gleissberg-Gnevishev’s minimum (1898-1923). Most probably the different type of oscillations in the sub-century and century period range corresponds to cycles of different classes of active regions. The solar-terrestrial relationships aspects of these results are briefly discussed.

Keywords: solar activity, solar cycles , extended solar data series

1. Introduction

The “conventional” point of view is that the solar flare events generally follow the overall sunspot activity. The typical picture is that the flare maximum in Schwabe-Wolf’s cycle follows 1.5-2 years after the main sunspot maximum.

Moreover, the correlation between the international sunspot index Ri and solar flares activity is far less convincing than for many others solar phenomena. As it is shown in Table 1 (Section 4), the relationship between the overall sunspot and flare activity is clearly falling down from the relatively weaker flare class C to the strongest class X (soft-X-ray flares classification, Crosby(2008)). The very high coefficient of correlation of +0.975 between Ri and the radio-index F10.7 indicates that more than 95% of the F10.7 changes follow this relationship during the last 30 years. On other hand, the coefficient of correlation between Ri and the strongest flare class X is + 0.449. This implies that only 25% of the X class flares could be related to the overall sunspot activity. That is an indication that the most powerful solar flares are caused by specific physical processes in the Solar atmosphere and their dynamics are very independent from the overall sunspot activity.

This conclusion agrees with the results in many recent studies. For solar cycle No 23 Killic (2009) found that no significant short-term periodicities (in the range close to a month) in the flare activity exist . The author pointed out a few_well expressed

cycles with duration between 23.1 and 36.4 days for the Ri data during the studied period. In a new study (Komitov and Duchlev, 2010- a study in progress) it is pointed out that the relative and absolute number of powerful solar flares of class X is essentially higher in the sunspot cycle No 20 than in the next two ones No 21 and 22, which are much stronger in the sunspot activity. It is also pointed out that the relative part of the powerful classes M and X is increased in the late phases of the sunspot cycles. Such solar cycle phase asymmetry has also been found for the related to the solar flares coronal mass ejections (CME) and Forbush decreases (Kane, 2008a). The sharp increase and extraordinarily high levels of flare activity during the so called “Halloween storms” (October-November, 2003) occurred during average levels of sunspot activity without any strong corresponding increase of Ri (Lilensten and Bornarel, 2006). Series of strong M- and X-class flares have occurred also in lower sunspot level conditions during 2004-2006.

These facts strongly stress the specific dynamics of the strong solar flares classes in comparison to the relative short time scales, of the order of the 11-year Schwabe – Wolf’s cycle or less. So, the assumption that in longer time scales (decadal, century or super-century) there could be significant differences between the sunspot Ri index and strong solar M and X classes dynamics seems very reliable. The problem of the long-term solar flares dynamics and their connection to other solar activity is very important. The understanding of that could help us better understand the physical conditions and generation of the strong flares and “mega-flares” like the “Carrington storm” from 1859 (Cliver, 2006) or the “Halloween storms” (October-November, 2003). A successful detection of statistically important long-term cycles, which are closely related to the flare activity could be also a starting point for building time series models and predictions for possible risk epochs of solar flares enhancement. The next very important question is: are there some long-term cycles and how stable they are?

The systematic observations of solar soft-X ray flares are provided since August 1975 as a part of the GOES satellites programs. There are additional earlier observations from March 1968, up to February 1973 by the SOLRAD satellite. The regular optical H-alpha flare observations are since 1936 (Link and Kleczek, 1949; Kleczek, 1952a). However according Kleczek (1952b) a serious lack of data during the World War 2 is possible in these data. There are homogenous data since 1976 published by the National Geophysical Data Center. A significant part of that data is based on the observations in the Skalnaté Pleso and Kandilli observatories and their analysis (Knoška and Petrásek, 1984; Ataç and Özgüç, 1998). Time series of the coronal mass ejections (CME) events connected to the solar flares are even shorter. Since the 1980^{ies} there are two relatively longer periods of regular CME observations: 1984-1989 (SMM satellite) and since January 1996 (SOHO satellite).

Thus there are not enough long instrumental series of direct flare observations for the clear establishing of long-term flare activity cycles with durations of 30-40 years or more. For the long-term tendencies it is necessary to use other solar or geomagnetical indices that could be considered as good proxies of the strong solar flare activity events. Such proxies for the century and super-century time scales could be the annual series of Groups sunspot number (AD 1610 -1995) (Hoyt and Schatten, 1998), as well as some historical or “synthetic” data like the Catalog of the Middle Latitude Aurora (MLA) events (AD 1000- 1900) (Křivský and Pejml, 1988), the simulated sunspot Rsi number and geomagnetic aa -index from the Extended time series of Solar Activity Indices (ESAI) (Nagovitsyn, 1997, 2006; Nagovitsyn *et al.* 2004). It is a fact that the most powerful solar flares could generate high energetic particles ($E \geq 100$ MeV). A part of the generated in the stratosphere “cosmogenic” isothopes atoms (^{10}Be , ^{14}C etc.) are of solar flare origin in addition to the main part, generated by the galactic cosmic rays (Usoskin *et al.*, 2006).

The strong quasi- 53-55, 60-67 and 115-120 years cycles have been found in the “Greenland ^{10}Be data series during the epoch AD 1423-1985 (Komitov *et al.*, 2003).

These results have been confirmed recently by Komitov and Kaftan (2004). A strong quasi 62-year cycle has been detected also in the time series of MLA-events from the catalog of Křivský and Pejml (1988) during the 18th and 19th century. The extrema are in very good coincidence with the corresponding extrema of the cycle with the same duration in the “Greenland” ¹⁰Be data (Komitov, 2009). The fact that the MLA events are connected to the flare activity of the Sun, including CMEs, suggests that a ~ 60-year cycle should exist in the solar flares dynamics, too. Weak, but statistically significant traces of 50-70 years cycles have been detected in Zurich (*Ri*) and Group sunspot number (GSN) series (Komitov and Kaftan, 2003). A strong “doublet” corresponding to cycles with durations of 114 and 144 years has been found in the synthetic north-south sunspot area asymmetry (Komitov, 2010). A similar result on the base of the analysis of Greenwich and Solar Optical Observing Network sunspot group data has been found by Javaraiah et al. (2005), who has determined its duration of 113 ± 5 years. A cyclic type trend, with a period of ~117 years has been also found in the Meudon solar filament series (AD 1919-1989) (Duchlev, 2001).

All these results indicate that there are solar activity processes for which the cyclic variations of ~50-60 and ~120 years are important features. They are related to the flares and corresponding active centers and sunspot groups rather than to the overall sunspot activity and the *Ri*-index.

The main aim of this study is a more detailed analysis of the problem of existence and stability of cycles with duration in the range of 20 – 250 years. The analysis uses different solar and geomagnetical data sets of instrumental and “historical” type. Two principally independent methods for time series analysis are used: a) the T-R periodogram analysis (standard (Komitov, 1986, 1997) and “moving window” regime (Bonev et al., 2004)); b) wavelet analysis (Torrence and Compo, 1998; Ranucci and Sello, 2004).

2. Data and Methods

For the purpose of this study, five sets of direct and indirect data series are used:

1. The mean annual Group sunspots number (*GSN*) (AD 1610-1995) (ftp://ftp.ngdc.noaa.gov/STP/SOLAR_DATA/SUNSPOT_NUMBERS/GROUP_SUNSPOT_NUMBERS/).
2. The international sunspot number *Ri* index series (AD 1749-2009) (ftp://ftp.ngdc.noaa.gov/STP/SOLAR_DATA/SUNSPOT_NUMBERS/INTERNATIONAL/)
3. The simulated international sunspot (*Rsi*) number from ESAI (AD 1090–2002) (Nagovitsyn, 1997, Nagovitsyn et al., 2004) (<http://www.gao.spb.ru/database/esai>)
4. The simulated geomagnetic *aa*-index from the ESAI (AD 1619–2003) (Nagovitsyn, 2006) (<http://www.gao.spb.ru/database/esai>).
5. The Meudon filament data series (AD 1919–1991). These data are taken from “*Cartes Synoptiques de la Chromosphere Solaire et Catalogues des Filaments et des Centres d'Activity: 1919—1989, published by Observatoire de Paris, Section de Meudon*” and for the period 1989-1991 from <http://bass2000.obspm.fr/lastsynmap.php>.

The first series (*GSN*) is taken as a better proxy of the solar short wavelength electromagnetic radiation and the corpuscular fluxes variability as the classical *Ri* – index. Unfortunately, it ends at AD 1995 and there are no plans for its continuation on this stage (Kane, 2008a).

The extended simulated sunspot series (*Rsi*) is the longest used in the present analysis – 913 years. The *Rsi*-series is based on the “historical” Schöve’s series (Schöve, 1955, 1983) for the moments of extrema and magnitudes of the Schwabe-Wolf sunspot cycles. The mean annual sunspot numbers there have been derived on the basis of Krylov-Bogolyubov’s approach to the description of weakly nonlinear oscillatory processes (Nagovitsyn, 1997; Nagovitsyn et al., 2004). It is important to note that the

original Schove's series is based predominantly on historical messages for auroral events and naked eye visible sunspots (i.e. potential sources of strong flares). By this reason it could be considered as a good proxy of the solar flare activity and its active centers. The *Rsi*- series has been analyzed in two stages : the last ~ 400 years since AD 1610 to compare with the *GSN*-series and the whole series (since AD 1090).

The length of the simulated *aa*-index (*AA*) is almost the same as the *GSN*. The Meudon filament series is relatively short and it is analyzed only with the standard T-R periodogram analysis. That series is not enough long for studying the evolution of cycles longer than the Schwabe-Wolf's cycle. However, it is included here as a proxy of the long-lived solar magnetic field structures .

Finally, the Zurich sunspot *Ri* annual series is used as an international standard for the overall sunspot activity.

Two preliminary procedures have been applied to all the studied time series:

1. Removing of general nonlinear trends (polynomials of second , third or fourth degree). The corresponding trend functions were obtained by the means of a least mean squares procedure. The best trend function expressions were determined on the basis of the best coefficients of correlations to the corresponding time series and the Snedekor-Fisher's *F*-parameter.
2. A smoothing procedure by 11 points (years) over the "residuals" was applied. The effect of Schwabe-Wolf's cycle has been removed and the signal of the long term cycles could be much better expressed.

We apply three type of time series analysis over these data sets.

A. The standard T-R periodogram procedure

The standard T-R periodogram analysis is used for searching for statistically significant cycles of the whole time series (Komitov, 1986, 1997; Benson *et al.*, 2003 etc.). This technique is very close to the algorithm, described by Scargle (1982).

The idea of this method is to approximate the studied time series $F(t)$ by minimized function $\varphi(t)$ of simple periodic type , i.e.:

$$F(t) \approx \varphi(t) = A_0 + A \cos(2\pi t/T) + B \sin(2\pi t/T) \quad (1)$$

where $t = 0,1,2,\dots$ are the corresponding moments in time step units (the time series step) . A_0 is the mean value of $F(t)$ based on the entire time series. T is the period , which is varied in range $[T_0, T_{max}]$ by step of ΔT . This way, a series of p minimized functions $\varphi(t)$ is obtained, where $p=(T_{max} - T_0)/ \Delta T$. The minimal possible value of T_0 is equal to 2 steps of the time series ($v=0.5$). For each one of the so obtained functions $\varphi(t)$ a correlation coefficient R to the time series $F(t)$ is calculated. The local maxima of R point to the possible existence of cycles with duration equal to the corresponding periods T .

The statistical significance of these cycles, based of ratio R/SR , is calculated ($SR = (1 - R^2)/\sqrt{N}$ is the error of R). A cycle is considered with more than 95% confidence, if $R/SR \geq 1.96$. N is the length (number of terms) of the time series. In addition, using a Monte-Carlo time series modeling, an essentially stronger criterion has been derived. It is necessary that $R/SR \geq 454/N^2 + 3.46$. For the long series, especially when N tends to infinity, R/SR tends quickly to 3.46. The last criterion arises from the fact that there are many cases of cyclic oscillations in pseudo-random number series, for which R/SR is between the two critical levels . In these cases, accepting the cycle could be based on additional expert criteria.

Since R depends on T , the series of $R(T)$ values obtained by the aforesaid procedure is labeled a "T-R correlogram" (Komitov, 1997).

As a criterion for the total magnitude of all oscillations in a range of periods $[T_1, T_2]$ on the basis of the T-R periodogram procedure, a quantity labeled “integral power index” S is given:

$$S = \int_{T_1}^{T_2} a(T) dT \quad (2)$$

Here

$$a(T) = \sqrt{A(T)^2 + B(T)^2} \quad (3)$$

is the amplitude of the corresponding minimized periodic function $\varphi(t)$ and $A(T)$ and $B(T)$ are determined by the mean least square procedure. For calculating S it could be taken $dT = \Delta T$.

The spectral resolution step used in the standard T-R periodogram calculations for the time series in this study is $\Delta T = 0.5$ years. T varies from 2 to 502 years, i.e. the T-R correlograms are calculated for 1000 different values of T .

B. “Moving Window” T-R Periodogram Procedure (MWTRPP)

The standard T-R periodogram procedure produces the mean parameters of the existing cycles in the time series. However, these cycles could significantly change between different parts of the time series. For studying a cycle’s evolution the so called “Moving Window T-R periodogram procedure” (MWTRPP) (Bonev *et al.*, 2004) is used. In this algorithm, a part of the time series of length P (“moving window”), where $P < N$ is defined. By author’s opinion it is recommended that $P / N \leq 1/3$ (Komitov, 2009). At the start of the procedure the “moving window” contains the first P terms of time series $F(t)$ and the standard T-R procedure is applied to those. After that the “moving window” is shifted with a step δT (one or more integer time series step), and the T-R procedure is repeated again, etc. Using this method, a series of T-R correlograms could be obtained, in which the y-coordinates corresponding to T values are presented as columns in two-dimensional maps, while the x-coordinates correspond to the central or starting moments of “moving window” epochs. In addition to R values, one could obtain maps of R/SR , $a(T)$ as well as the evolution of the coefficients $A(T)$ or $B(T)$.

The “moving window” in our MWTRPP- procedures have been chosen to be $P = 150$ years. We used a variable ΔT that is a step for the T-R correlogram of the separated “moving window” epochs. The step was increased by a factor of 1.01 between the adjacent periods T , so that it corresponds to the power law $T_m = T_0 \times 1.01^m$, where m varies from 0 to 249. T_0 is chosen to be 20 years and thus $T_{max} = T_{249} \approx 240$ years. Clearly, the condition $P > 1.5T_{max}$ is not satisfied. However, we make this compromise taking into account the fact that the most of studied series are relatively short ($N \leq 400$ years) and a choice of larger value for P would make the MWTRPP-method non-effective for these series, most notably for Ri (the Zurich series). On other hand the range about ~200 years is interesting in view of the fact that there are many evidences for the existence of a strong solar cycle there (Schöve, 1955, 1983; de Vries, 1958; Stuiver and Quay, 1980; Damon and Sonett, 1991; Dergachev, 1994; Komitov and Kaftan, 2003; Bonev *et al.*, 2004). Thus, the results should be fully certain for the range of cycles shorter than 100 years, satisfactorily certain for $100 \text{ years} \leq T \leq 150 \text{ years}$, while for longer ones ($T > 150 \text{ years}$),

they should be taken only as a rough guide. The single shifting (scan step) of the “moving window” is 1 year.

C. The wavelet- analysis

This technique has been extensively applied in complex nonlinear time-series analysis, including the study of solar and stellar activity cycles (Torrence and Compo, 1998; Sello, 2003; Ranucci and Sello, 2004). With a local decomposition of a multiscale signal, wavelet analysis is able to properly detect time evolutions of the frequency distribution. This is particularly important when we consider intermittent and, more generally, non-stationary processes. More precisely, the continuous wavelet transform represents an optimal localized decomposition of a real, finite energy, time series: $x(t) \in L^2(\mathfrak{R})$ as a function of both time t , and frequency (scale), a , from a convolution integral:

$$(W_{\psi} x)(a, \tau) = \frac{1}{\sqrt{a}} \int_{-\infty}^{+\infty} dt x(t) \psi \left(\frac{t - \tau}{a} \right) \quad (4)$$

where ψ is called analysing wavelet if it verifies an admissibility condition:

$$c_{\psi} = \int_0^{+\infty} d\omega \omega^{-1} |\psi(\omega)|^2 \quad (5a)$$

with

$$\psi(\varphi) = \int_{-\infty}^{+\infty} dt \psi(t) e^{-i\omega t} \quad (5b)$$

This last condition imposes: $\hat{\psi}(0) = 0$, i.e. the wavelet has a zero mean. In (4); $\tau \in \mathfrak{R}$; ($a \neq 0$) are the scale and translation parameters, respectively. In fact, it follows from (4) that the effectiveness of the wavelet analysis depends on a suitable choice of the analysing wavelet for the signal of interest. For our time-series application, where we are mainly interested in tracking the temporal evolution of both the amplitude and phase of solar activity signals, we chose to use the family of complex analysing wavelets consisting of a plane wave modulated by a Gaussian, called Morlet wavelet (Torrence and Compo, 1998):

$$\psi(\eta) = \pi^{-1/4} e^{i\omega\eta} e^{-\eta^2/(2\sigma^2)} \quad (6)$$

where: $\eta = (t - \tau) / a$, and ω_0 is a non-dimensional frequency. σ is an adjustable parameter which can be determined in order to obtain the optimal wavelet resolution level both in time and frequency, for the characteristic time-scale of the original series. The limited frequency resolution imposes a half-power bandwidth of our wavelet given by $\Delta f / f \approx 0.12$. The principal information derived from the application of the wavelet formalism to real data is the wavelet local spectrum, which allows us to resolve the multiscale time-evolution of the related frequency distribution.

3. Results and analysis

3.1 The Zurich series (1750-2009)

As it is shown on Figure 1 where the T-R correlogram is plotted, the main long-term cycle in the international sunspot number Ri series is approximately 95.5 years long. The corresponding peak of the correlation coefficient R exceeds its error 18.8 times. The “zero- hypothesis” probability in this case is $\ll 10^{-6}$. Consequently, the quasi-centennial cycle should be considered as the most important feature of the international sunspot index Ri , after the 11-year Schwabe- Wolf’s cycle. The second clear visible long-term oscillation has $T= 58.5$ years. The corresponding R/SR ratio is also very high (~ 8.8) and with significance $> 99.999\%$, i.e. “zero-hypothesis” level is less than 0.001% . There are also traces of 41-year and 29-year oscillations that are weaker, but with high statistical significance.

The MWTRPP amplitude map of the Zurich series is shown on Figure 2. An evolution of the quasi-centennial oscillation during the last 260 years is clearly visible. During the first 150 years, i.e. the second half of 18th and the 19th centuries this cycle is noticeably shorter (~ 70 years). However, during the next decades its duration is slowly increased and in the 20th century it is already slightly longer than 100 years. The calendar centres of the moving window epochs when the quasi-centennial cycle is better expressed are near to AD 1825 (the Dalton minimum) and AD 1870.

There is no good trace of a ~ 55 -year cycle during the 18th century. As it is shown, this cycle is in process of “separation” from the quasi century oscillation during this time. The ~ 55 -year cycle is well expressed in the 19th century up to AD 1870, but after that it is falling down both in amplitude and duration. A new increase in the amplitude is observed in the 20th century, but now the cycle length is about 40-42 years. On other hand, a quasi 42-44 years cycle is very well expressed in the middle of the 19th century almost simultaneously with the 55-year one. Another visible weak oscillation is the quasi 30-year cycle (~ 3 Schwabe-Wolf’s cycles). Its amplitude has increased and decreased three times during the whole period of 260 years. The last one corresponds to the recent decades.

The results from the wavelet-analysis (WA) are shown in Figure 3. The strongest cycle here has a duration of ~ 94 years. It is slight shorter during the 18th century with a weak tendency of prolongation during the 19th and 20th centuries is observed. In the recent part of the series (20th century) this cycle tends to a duration of ~ 100 -110 years. The second by importance cycle is the 54-year one. It is very well expressed in 18th and 19th centuries. After \sim AD 1850 its amplitude is fading.

3.2 The Group sunspot number series (1610-1995)

According the results from the T-R periodogram analysis the main cycle in the GSN series during the last ~ 400 years is with quasi-two-century ~ 202 years duration (Figure 4). The corresponding coefficient of correlation R is ~ 0.58 . The second by significance ($R= 0.52$) is the 108-year cycle. There is also a quasi 80 years oscillation. The subcentennial 54-year cycle is the next significant oscillation ($R= 0.33$). There are also very weak traces of 28- and 21.5-year cycles. The ratio R/SR for the last two ones is in the range of 2.0 to 3.5.

On the base of MWTRPP-method we found that the quasi-two-century oscillation was very powerful during the 17th and 18th centuries, i.e. during the Maunder minimum and the first decades after that. However, since the Maunder minimum it quickly fades and is transformed to shorter duration. Close to the Dalton minimum (1795-1830) there are no more visible cyclic tendencies of a century or longer duration. The main long term cycle at the end of the Dalton minimum has a period of about 70-75 years. After the Dalton minimum, a slow prolongation starts for this cycle and its “actual” length during the 20th century is approximately 110 years.

A relative stable 50-60 years cycle is clearly visible in Figure 5 for almost the entire GSN data series. This cycle is best expressed in the 18th and 19th centuries up to AD 1870, and in the 20th century it is significantly weaker. During the last decades a weak quasi 30 year cycle appeared.

According to the wavelet analysis the quasi ~200 year cycle is most powerful in the earlier part of GSN series (Figure 6) Its amplitude slightly falls from the 17th to 20th centuries. In contrast, a cycle with duration of ~110 year increases in amplitude during this time. Another ~80-year oscillation, which exists during the 17th and 18th centuries is quickly converges to the 110-year one approximately after the Dalton minimum. A 54-year cycle exists in the whole series, but it is most powerful during the 18th and 19th centuries. The peak of its amplitude is near AD 1820. As in the MWTRPP-map (Figure 5) a 30-33 years cycle is well visible in the most recent part of the GSN-series.

As in the case of *Ri* (Zurich series), the wavelet amplitude spectra of *GSN* (Figure 6, right) is very similar to the corresponding T-R correlogram (Figure 4).

3.3 The simulated sunspot *Rsi* series (1600-2002)

The results from the analysis of the extended sunspot *Rsi* data series from ESAI since AD 1600 are shown in Figures 7, 8, and 9. The quasi-two-century cycle is ~198 years according the standard T-R correlogram (Figure 7) or ~ 206 years from the wavelet amplitude spectra (Figure 9, right). There is also ~ 115 –120 years cycle (116.5-year by T-R analysis – Figure 7; 119-year in the wavelet spectra - Figure 9, right). An 80-83 years cyclic oscillation is found as well. By the both methods a ~55-60 years cycle ranks third in magnitude. As in the *Ri* and the *GSN* series, a weak ~29-year oscillation is detected in the simulated *Rsi* data set.

As in the *GSN* series, there is a tendency for fading of the quasi-two-century cycle. The cycle is very sharp after the Maunder minimum according the MWTRPP (Figure 8) and very gradual according the wavelet method (Figure 9).

By the MWTRPP the quasi 115—120 years cycle stays important after the Dalton minimum. According to the WA study this cycle is presented in the whole series, but it is quickly growing in amplitude at the beginning of the 20th century, when the relative weak 80-85 years cycle has been “attached” to it. This moment corresponds approximately to the century’s Gleissberg-Gnevishev’s minimum (AD 1898-1923).

The 55-60 years cycle exists in the entire *Rsi*- series, but it is weak during the Maunder minimum and the modern epoch. The times when it is best expressed are during the 18th and 19th centuries.

According to the MWTRPP there are traces of ~30 and 40-45 years cycles for the duration of the entire *Rsi* series. However, the amplitudes of these cycles are higher during the 20th century (Figure 8). The wavelet analysis shows that the quasi 29-30 years cycle is well expressed at the end of the 20th century plus a short local peak at the beginning of it, but it is totally absent before the Dalton minimum (AD 1795-1830)(Figure 9).

3.4 The simulated *AA*-index series (AD 1619-1999)

The length of the simulated *aa*-data series from ESAI used here is almost the same as that of the *GSN*-series (381 years). The signature “AA” is used in this work to distinguish it from the instrumental *aa*- index. The study of this series is very interesting because of the possibility for comparison of the results of this pure “geophysically oriented” series to the other ones, which are related to the sunspot active centers.

According to MWTRPP the quasi 55-60 years cycle is very stable in the earlier and middle part of the series (Figure 11) and it is slightly better expressed in the *AA* than in the *GSN* and *Rsi* series. On other hand the WA results reveal that this cycle is even

better expressed during the 17th century in AA (Figure 12) than in the cases of *GSN* and *Rsi*.

There is a hint of a better expressed quasi 30-year oscillation during the earlier part of the AA-series (Figures 11 and 12). According to the WA the higher amplitudes of this cycle are at the end of the 20th century (Figure 12), while as follows from MWTRPP, the absolute amplitude peak of the quasi 30-year oscillation occurs almost a century earlier (Figure 11).

3.5 The Meudon filament data series (AD 1919-1991)

Unlike the other data sets investigated here, the smoothed filament series of the Meudon observatory catalog is relatively short, covering only 61 years. For this reason, it is not possible to effectively search it for any cycle evolution in the multidecadial range. Therefore, we study only the mean features of the whole series and mainly on the base of the standard T-R periodogram analysis (Figure 13). As it is shown, there are 66.5-, 26.5- and 17.5-year cycles. The WA-test gives, due to the shortness of this time series, only a weak 26.5-year cycle (Figure 14).

These results are interesting due to the fact that the filaments are a relative “pure” indicator for the coronal activity phenomena. The existence of 66.5-year cycle is evidence that the subcentury periodicity is real for these events at least during the 20th century. The absence of quasi 117-year cycle, which was detected earlier by Duchlev (2002) could easily be explained by the de-trending procedure.

3.6 The long term solar cycles during the last ~900 years

The time series used in Sections 3.1-3.5 are relatively short. They all begin near, or after the supermillennial Maunder minimum (AD 1640-1720). Moreover, they are almost entirely contained within a period of a long term upward trend of the solar activity, during the initial active phase of the quasi-bimillennial solar 2200-2400 year cycle (Hallstadtzeit) (Damon and Sonett, 1991; Dergachev and Chistyakov, 1993; Bonev et al., 2004). As it has been already demonstrated by some of these authors (Damon and Sonett, 1991; Bonev et al., 2004) on the basis of ¹⁴C data, as well as by Komitov et al. (2004) (¹⁴C and Schove's series), Maunder-type minima are not only the starting phases of Hallstadtzeit cycles. Serious changes of the solar activity dynamics occur during these epochs. The amplitudes of the quasi two-century cycles (~170-220 years) fade, while in their place an increase of the cycles by quasi-century duration begins. This suggests that it is interesting to search for the stability and evolution of the cycles from the studied range over longer than 400 years time scales. It is especially interesting to investigate how the transition from the previous Hallstadtzeit cycle to the present one affects the solar oscillations with sub-century periods (20-70 years).

For this purpose, we use the whole *Rsi* simulated data series from the ESAI. As it has been already noted in Section 2, this series starts from AD 1090 to 2002 and contains annual data for 913 years. The T-R periodogram analysis is used both in its standard and MWTRPP versions. The “moving window” length P is 400 years. All other parameters are the same as those described in Section 2. As for the other series, the trend is removed and an 11 years smoothing procedure has been performed. The larger width of the window P provides much better conditions for the MWTRPP than in Sections 3.1-3.4 over all and especially in the range of $T \geq 150$ years. The results are shown on Figures 15, 16 and 17.

The main cyclic oscillation in sunspot activity during the last ~900 years is with duration of 204 to 209 years (Figures 16 and 17). According to Figure 15 there is a ~121.5-year cycle and an oscillation with duration of 82 years, i.e. very close to the so-called “Gleissberg cycle” (78 years) (Gleissberg, 1944). There is also a very well expressed 59.5-year cycle. A weaker cyclic component at $T=54$ years is also present. Weak

signatures of 41- and 29-year cycles are found, which are near or even less than the critical level $R/SR= 3.46$.

As it is shown on Figure 16 the quasi 200-year cycle is very significant before the Maunder minimum epoch. The absolute maximum of its amplitude corresponds to the calendar center of the 400 years window at ~AD 1550. This epoch contains both of the deepest solar supercentury minima during the last 2000 years - those of Spörer (AD 1400-1520) and Maunder (AD 1640-1720). This result matches very well all other previous evidence, that during the Hallstadzeit cycles minim, the amplitude of the quasi two-century cycle tends to a maximum, while the quasi-century ones – to their absolute amplitude minima (Damon and Sonett, 1991; Bonev *et al.*, 2004; Komitov, 2007). According to the WA results (Figure 17) the amplitude of the ~200 yr cycle tends to reach a maximum near the Spörer–Maunder minimums epoch , but the fading after that is less pronounced than in Figure 16.

The relative fading near the Maunder minimum (moving window calendar center at ~AD 1600) of all cycles by duration 40-140 years is well pronounced in Figure 17. But it should be noted that in the entire period of 11th- 20th centuries, three very stable oscillations in the subcentury and quasi century range are always present, corresponding to mean periods of 55-60, ~80 and ~ 120 years. They could be followed in Figure 16 during the entire ~900-year period. One could conclude that there is no general mean quasi-century cycle during the last millenium, but rather quasi centurial doublet ($T= 80$ and 110-120 years) or triplet if the subcentury 50-60 years cycle is also considered.

The amplitude of the longest ~120-year component reaches local maxima near the 11th , 15th and 20th centuries. The behavior of the ~55-60 years cycle is also interesting. The epochs of its higher amplitudes are after the Maunder minimum, as well as in 11th-12th centuries. Between the 12th-17th centuries the amplitude of the 55-60 years oscillation remains significant , but not so high.

It is shown on Figures 16 and 17 that unlike the quasi-century multiplet (50-60, 80 and 120 years) the shorter cyclic variations are not stable on longer time scales. There are only weak traces of the 40-45 year cycles predominantly before the Maunder minimum and during the 20th century (Figure 16). Traces of the ~30-year (~3 Schwabe-Wolf's cycles) oscillation are even weaker and sporadic. As can be seen, the ~30-year cycle is slightly better defined during the latest part of the series and mainly due to its significant increase in amplitude during the 20th century (Figure 16 and 17).

It is interesting to note that near the Maunder minimum, significant traces of ~35-38 years cycle are visible in Figure 16 (the MWTRPP map) . An oscillation with such duration has been detected for the period of AD 1932-2005 in the annual number of the strongest geomagnetic storms, when the A_p -index exceeds 40 (Komitov, 2008).

4. Discussion

The results presented in Section 3 provide clear evidences that there are three significant and relatively stable quasi-oscillations during the last millenium with sub- and quasi-century duration. Their durations are of 55-60, ~80 and 110-120 years, respectively. As it has been shown in Sections 3.1-3.4 both by the WA and the MWTRPP methods their periods are slightly variable in the shorter time scales, for example the epoch of instrumental observations, i.e. the last ~400 years. On other hand, the MWTRPP test over the entire Rsi series shows that the reliable presence of this quasi-century multiplet covers the whole ~900-year period if a larger smoothing window is used.

However, as is shown in Figures 2, 3, 5, 6, 8, 9, 11, 12, and 17, the ratios between the amplitudes of these three oscillations are different in the different epochs. This could explain why there are serious variations in the length of the observed quasi-century cycle in the different epochs. Gleissberg (1944), found a length of ~78-80 years. In his study, the data used referred to sunspot cycles No 0-17, when the ~110-120 year

component is noticeably weaker. Thus, the ~94-95 years century cycle in the whole Zurich series (Figures 1 and 3) is only a “mean-weight” one and it is an integral result of the more important role of the 55-80 years and the ~80-year cyclic components in the earlier part of this series and the fading and increasing of the ~120-year component in the recent part of the series.

On the other hand, the 50-60 years cycle is strong only in the first half of this period (before ~AD 1870), but it is interrupted after the Gleissberg-Gnevishev minimum epoch (1898-1923). However, the strengthening of the ~120-year component and the weakening of the 80-year one after the Dalton minimum and during the 20th century is the cause for the delay of the next long-term minimum. That minimum began not after the end of solar cycle No 21 in AD 1986, but about 20-22 years later, i.e. at the end of cycle No 23. The imminent long-term minimum in the first half of the 21st century has been predicted by many authors (Fyodorov *et al.*, 1995; Badalyan *et al.*, 2000; Komitov and Bonev, 2001; Komitov and Kaftan, 2003; Shatten and Tobiska, 2003; Solanki *et al.*, 2004; Ogurtsov, 2005; Cliver *et al.*, 2006). As a consequence of that, the amplitude of solar cycle 24 is expected to be relatively low ($Ri_{max} \sim 90$). (Pesnell *et al.*, 2009).

The complicated structure of the quasi-century cycle was established as early as Schöve (1955) on the basis of historical records of auroral events for the last ~2000 years. In addition to the Gleissberg (~78 years) cycle, he found that there are also tracks of longer (~120-130 years) or shorter (54-55 or 65 years) oscillations.

It is very probable that the three distinct components of the quasi-century multiplet are connected to the long-term dynamics of different classes of active centers and sources of flare activity. On the basis of Křivský and Pejml (1988) catalogue data Komitov (2009) found that a strong 62.5-year cycle exists in the annual numbers of middle latitude aurora (MLA) events during the 18th and 19th centuries. In this study they also find that the peaks of this auroral cycle correspond very well to the quasi 60-year cycle maxima of ¹⁰Be production rates in the “Greenland” beryllium-10 data series (Beer *et al.*, 1990, 1998).

It is interesting to note three additional facts here, namely: 1. The 11-year cycle is weak in the T-R spectra of MLA annual number (Komitov 2009b), while the 62.5-year one is very strong (the corresponding peak in the coefficient of correlation R is ~0.65). This result was found without the application of any smoothing procedure. 2. There are closely coinciding peaks both in the MLA and the ¹⁰Be production rates near AD 1725-1735, ~1800-1805, and 1865-1870 (there is a slight delay in ¹⁰Be in the range of 3-5 years, which could be explained by the “resident time” (Damon *et al.*, 1997)). 3. The annual number of MLA events has drastically decreased after AD 1870 when the 50-60 years cycle in Ri , GSN , AA , and Rsi is weaker (Figures 2, 3, 5, 6, 8, 9, 11, and 12).

The MLA phenomena are associated usually with strong solar flare events, which also cause coronal mass ejections (CME). Thus, taking into account the aforementioned three facts it could imply that the 50-60 years cycle is a feature of these active solar centers, which are the typical sources of strong flares and CMEs. The coincidence of the local peaks in the 60-year cycles of ¹⁰Be and the MLA during the 18th and 19th centuries suggests that a significant fraction of the ¹⁰Be atoms could be produced in the stratosphere by highly energetic particles from strong solar flares (Usoskin *et al.*, 2006). This could make the relationship between the sunspot activity and ¹⁰Be production rates much more complicated on century or subcentury time scales compared to the case of only a pure Forbush-effect (Komitov, 2009).

There could be another point of view on the possible relation of the 50-60 years cycle to the sources of the strongest solar flares. It concerns the historical data for giant, naked eye visible sunspots and sunspot groups. As was shown by Vaquero (2002, 2007), there are three peaks of the 50 years smoothing annual numbers of the giant sunspots during the 18th and 19th centuries, near to AD 1735, AD 1805, and AD 1870. These three peaks correspond very closely to the ~60 years maxima of the MLA annual number and the “Greenland” ¹⁰Be concentrations data. The strong downward trend in the annual

number of giant sunspots after AD 1875 coincides well both with the corresponding downward tendency of MLA (Komitov, 2009) and the amplitude of the 55-60 years oscillation (Figures 2, 3, 5, 6, 8, 9, 11, and 12 in Section 3). Thus, it is very probable that the 55-60 years cycle in the sunspot activity is connected directly to the active regions, which are the sources of the strongest solar flares, corresponding to the X-ray classes M and X.

Vaquero (2007) shows that there is no significant correlation between the *GSN* (i.e. the overall sunspot activity) and the visible by naked eye sunspots at all. On the contrary, there is a significant anticorrelation or non-correlation over large fractions of this period. It is also evident from Figures 16 and 17, that the amplitude changes of the 55-60 years cycle are the most independent relative to the two other components of the quasi-century multiplet. Let us also take into account the very small amplitude of the Schwabe Wolf's cycle in the MLA events (Komitov, 2009). By combining and comparing all these facts, we arrive at the conclusion that these active centers, which are related to the most powerful flare classes and are subject to the 55-60 years cycle are relatively independent of the overall sunspot activity dynamics. Thus, the weak correlation between X and M class flares and the overall sunspot activity Ri during the last 35-40 years (Table 1) is a consequence of the same weak relationship on long time scales.

Table 1. The coefficients of linear correlation between the monthly values of 6 solar and solar-modulated indices for the period January 1980 - December 2009

	Ri	$F107$	$Nflux$	N_C	N_M	N_X
Ri	1	0.975	-0.798	0.847	0.719	0.449
$F107$	0.975	1	-0.796	0.856	0.759	0.487
$Nflux$	-0.798	-0.796	1	-0.724	-0.615	-0.464
N_C	0.847	0.856	-0.724	1	0.672	0.415
N_M	0.719	0.759	-0.615	0.672	1	0.770
N_X	0.449	0.487	-0.464	0.415	0.770	1

Ri - the international sunspot number

$F107$ - solar radioflux at $f=2800$ MHz ($\lambda=10.7$ cm)

$Nflux$ - GCR neutron flux (Moscow)

N_C , N_M and N_X - monthly numbers of X-ray flares of C, M and X classes by GOES satellite data

There are some other interesting studies, concerning the existence of solar cycles with duration of quasi-3 (Ahuwalia, 1998) and quasi-5 (Du, 2006) Schwabe-Wolf cycles, i.e. 30-33 (three cycle periodicity, the so called "TRC-rule") and ~ 55 years, respectively. The existence and stability especially of the TRC has been analyzed critically by Kane (2008b). He has found that there are only three sequences of Schwabe-Wolf cycles during the last 300 years, for which the TRC-rule is valid and two of them covered the Zurich cycles No 17-22. On the other hand, the quasi-4 Schwabe-Wolf's cycle periodicity (~40-45 years) has been detected in the north-south asymmetry of the sunspot area by Javaraiah (2008) and Komitov (2010).

In the present study, we found that the ~30 and 40-45 years oscillations are present in separate epochs in the overall sunspot and geomagnetic activity, but in contrast to the century multiplet components, they are very unstable and weak. However, both cycles have significantly higher amplitude in the recent epoch. Most probably the observed TRC-rule for the Zurich cycles No 17-22 is not connected to this event (Figures 8 and 11). How the increasing of the ~30 yr cyclity is related to the supercentury solar activity dynamics and especially to the 2200-2400 years Hallstadtzeit cycle is an interesting question, which needs a special study.

It is necessary to note that there is no strong correspondence between the observed ~30- year cycle and the "TRC-rule". The ~30-year cycle in our study is a feature of the absolute amplitude variations of the smoothed and de-trended series of solar indices, while the "TRC-rule" describe a relative relationship between three consecutive 11-year Schwabe-Wolf's cycles.

As we have already noted, the ~200-year cycle is one of the main features of the solar activity on the supercentury time scale. We found here that this cycle has been very powerful before the Maunder minimum and obviously weaker after that. Its decreasing amplitude during the last ~400 years of instrumental observations is detectable, but it is quite gradual according to the WA-method. However, this fading is abrupt according the MWTRPP procedure. This is caused by the use of relatively narrow “moving window” ($P=150$ years) for studying the shorter series (Figures 2, 3, 5, 6, 8, 9, 11, and 12), which make the method not precise enough for cycles of the same or longer duration. On the other hand, an additional disturbance over the ~200-year cycle is caused by the Gleissberg-Gnevishev’s minimum (1898-1923). The detected dynamics of the 200-year cycle match previous results and conclusions about its amplitude modulation by the Hallstattzeit cycle (Damon and Sonett, 1991; Bonev *et al.*, 2004; Komitov *et al.*, 2004).

The comparison of Figures 2, 3, 5, and 6 shows that there are no significant differences in the cyclic oscillations of the Zurich (Ri) and GSN series in their general part after AD 1750. This fact could be easily explained. The main differences between the two series are related to the general trend in the earlier part, near and before the Dalton minimum, when the Ri series is overestimated according Hoyt and Schatten (1998). However by first removing the general trends in the two series, this difference is removed as well.

5. Conclusions

By applying the essentially independent methods of the T-R periodogram analysis, both in the standard and “moving window” regime, and the wavelet analysis on five different solar and geomagnetical data sets a detailed analysis of the problem of the existence and stability of cycles with duration in the range of 20 – 250 years was made. On the basis of the results obtained in this study, the following main conclusions can be made:

1. The quasi century cycle in sunspot and geomagnetic activity has a complicated multiplet structure, which is clearly detected in different types of instrumental and simulated indirect data on supercentury time scales (~400 years or longer). There are three important and relatively stable components of this multiplet with durations of 55-60, ~80 and ~120 years, respectively. Most probably they are related to different types of solar active centers and sunspot groups. The Gleissberg’s ~78-80 years cycle is only one of these components.

2. There is a tendency during the last ~150 years towards increasing the amplitude of the quasi 120-year cyclic component and fading of the ~80-year one.

3. It is very probable that the quasi 50-60 years cycle is related to the sources of the most powerful solar flare events (x-ray classes M and even more X) and CMEs. They are relatively independent from the overall sunspot activity dynamics and the 11- year Schwabe-Wolf’s cycle. Their relative participation in the overall solar and geomagnetic indices is low.

4. The quasi 40-45 and 30 years cycles in the solar and geomagnetic activity indices are unstable during the long time scales and their amplitudes are low. A visible strengthening of the quasi 30-year periodicity during the last few decades is observed.

5. There is no essential difference between the cyclic dynamics of the Group sunspot numbers (GSN) and Zurich series (Ri - index) since AD 1750 if the general trends from both series are removed.

Acknowledgements

The authors are grateful to Prof. Yu. Nagovitsyn for his help with compiling the data from ESAI (<http://www.gao.spb.ru/database/esai>). The authors are thankful to the National Geophysical Data Center, Boulder, Colorado, U.S.A. for providing the annual Group sunspots number and international sunspot number data via <ftp://ftp.ngdc.noaa.gov/STP>, and the Meudon Observatory, Paris, France for providing the filament number data via <http://bass2000.obspm.fr>.

Institute of Astronomy, 72 Tsarigradsko Chaussee, Sofia 1784, Bulgaria
b_komitov@sz.inetg.bg
duchlev@astro.bas.bg
mdechhev@astro.bas.bg
koleva@astro.bas.bg

Stefano Sello

Mathematical and Physical Models, Enel Research, Via Andrea Pisano 120, 56122 Pisa - Italy

Kaloyan Penev

Harvard University, Mail Stop 10, 60 Garden Street, Cambridge, MA 02138
e-mail: kpenev@cfa.harvard.edu

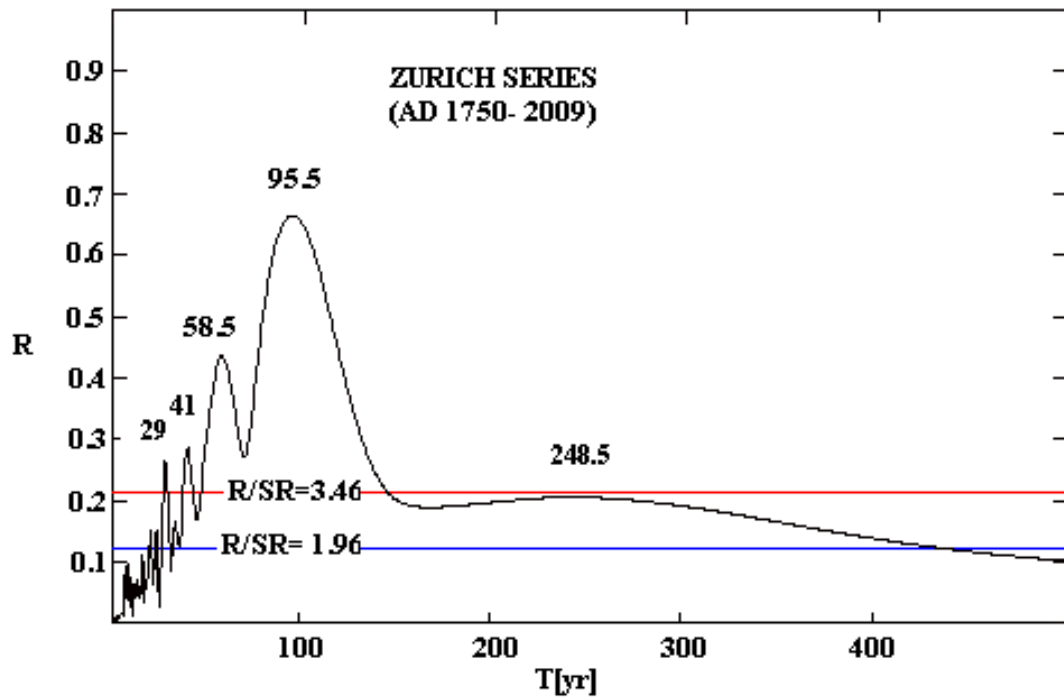


Fig. 01 T-R corellogram of the Zurich series (AD 1750-2009)

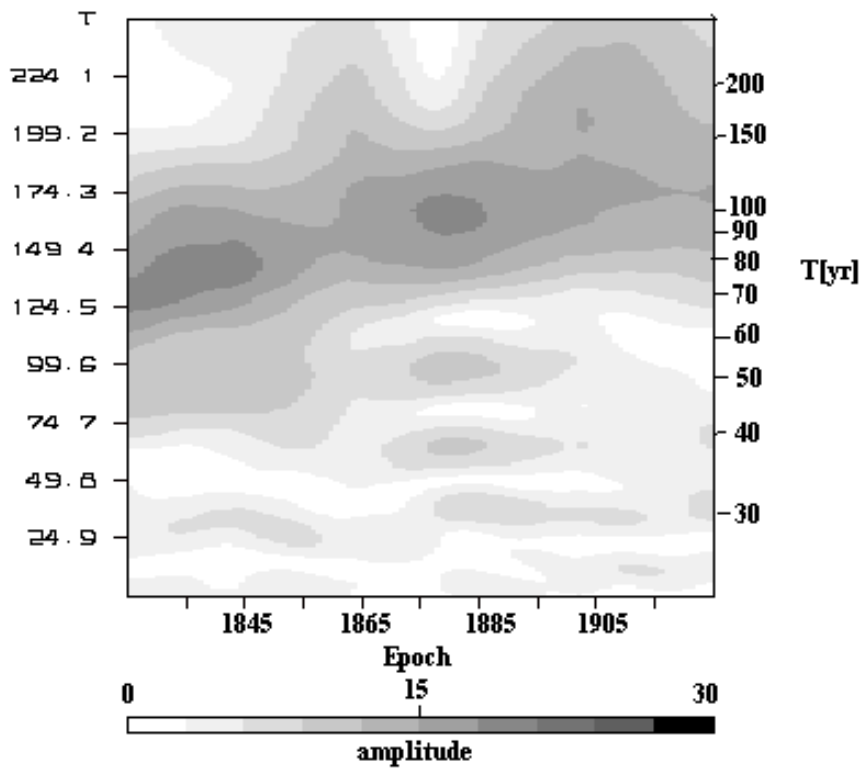


Fig. 02 MWTRPP amplitude map of the Zurich series (AD 1750-2009)

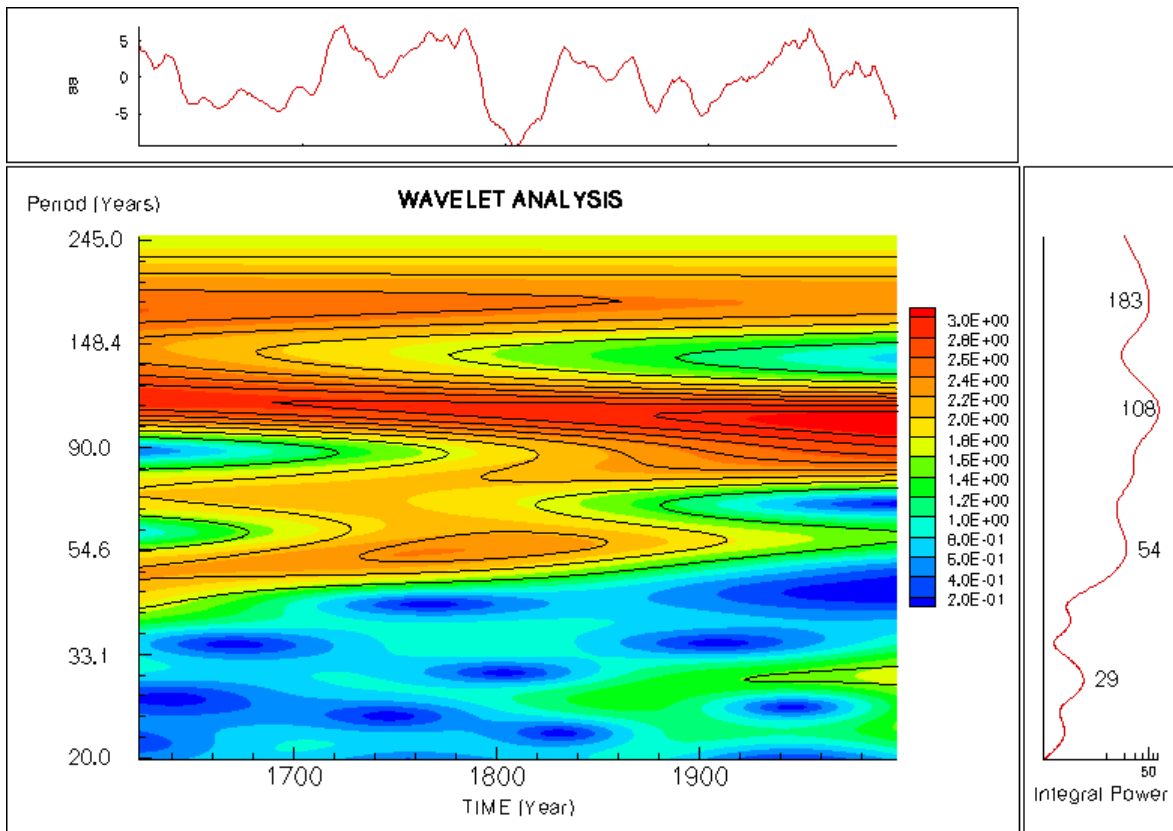


Fig. 03 WA amplitudes of the Zurich series (AD 1750-2009)

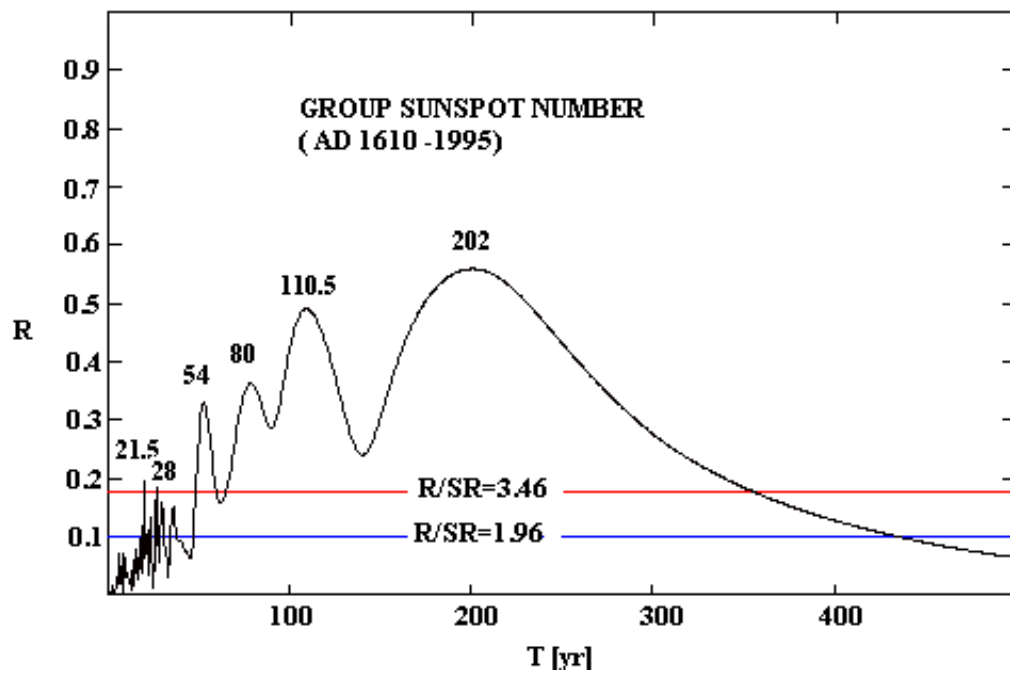


Fig. 04 T-R corellogram of the Group sunspot number (GSN) series (AD 1610-1995)

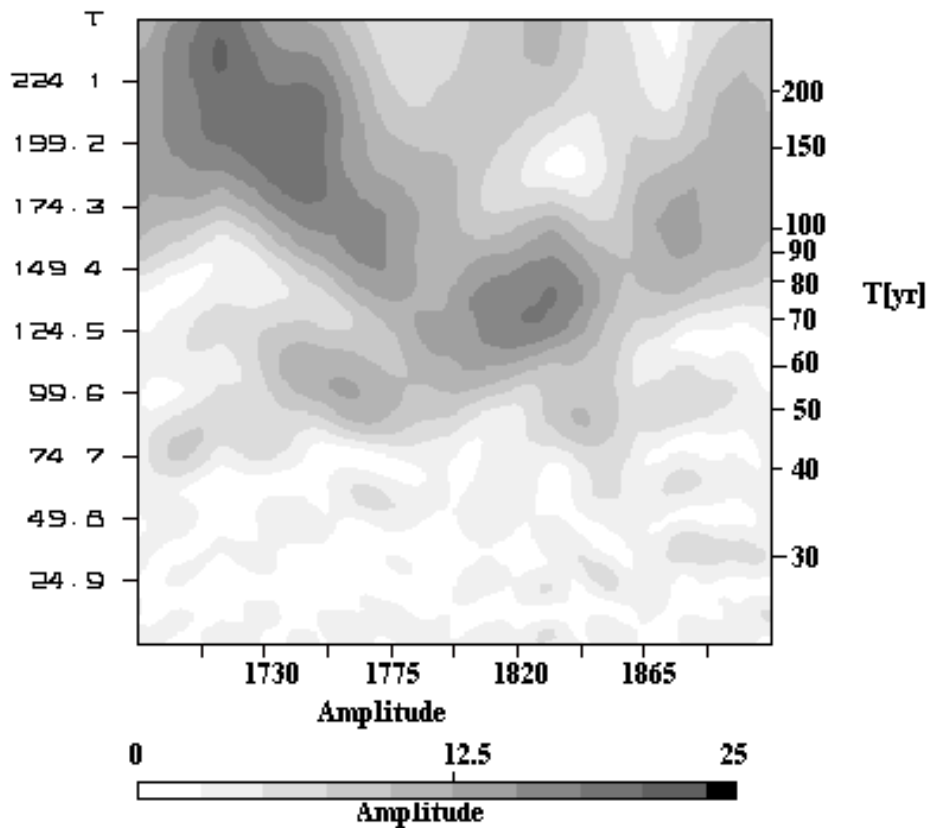


Fig. 05 The MWTRPP amplitude map of the Group sunspot number (GSN) series (AD 1610-1995)

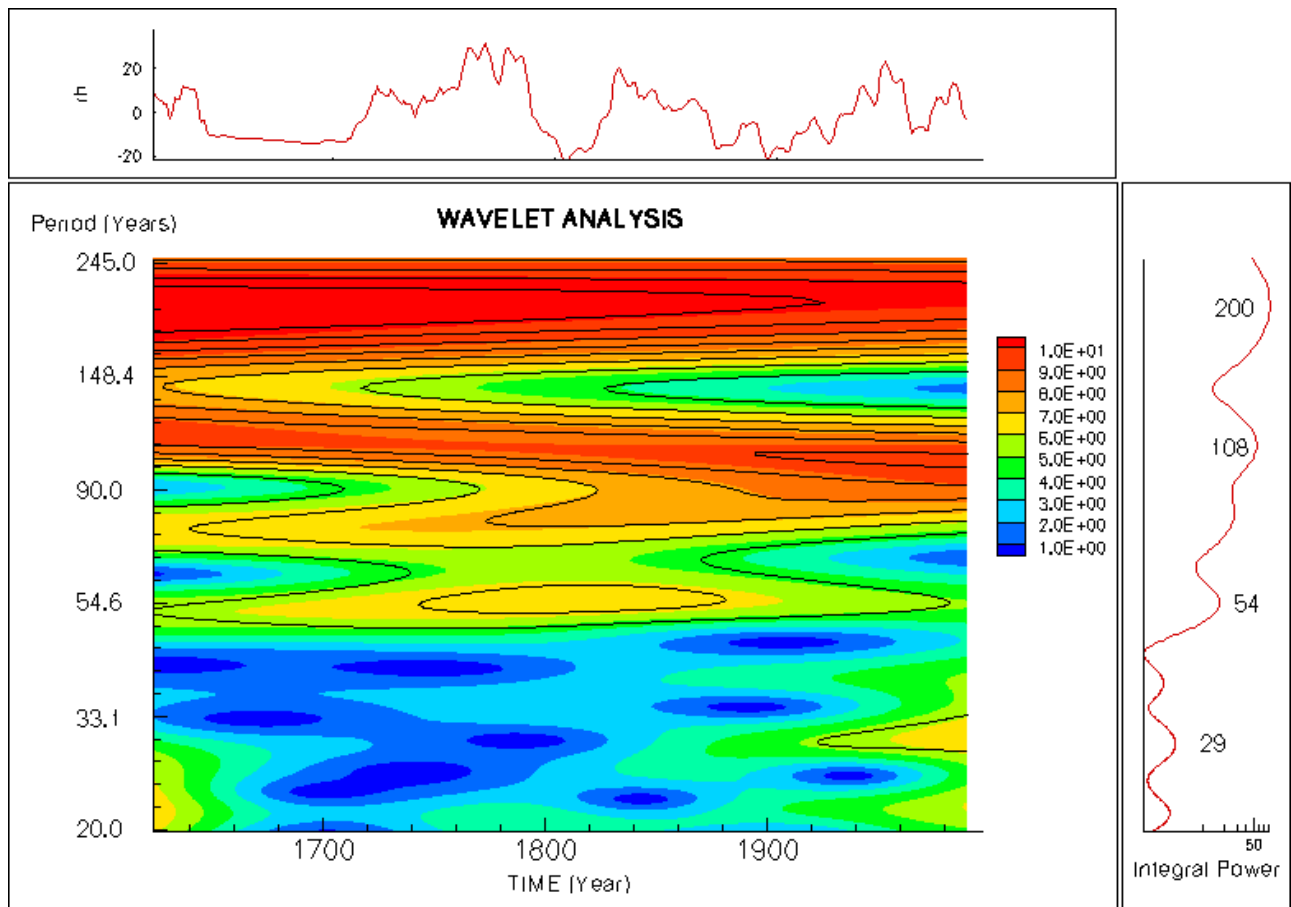


Fig. 06 WA amplitudes of the Group sunspot number (GSN) series (AD 1610- 1995)

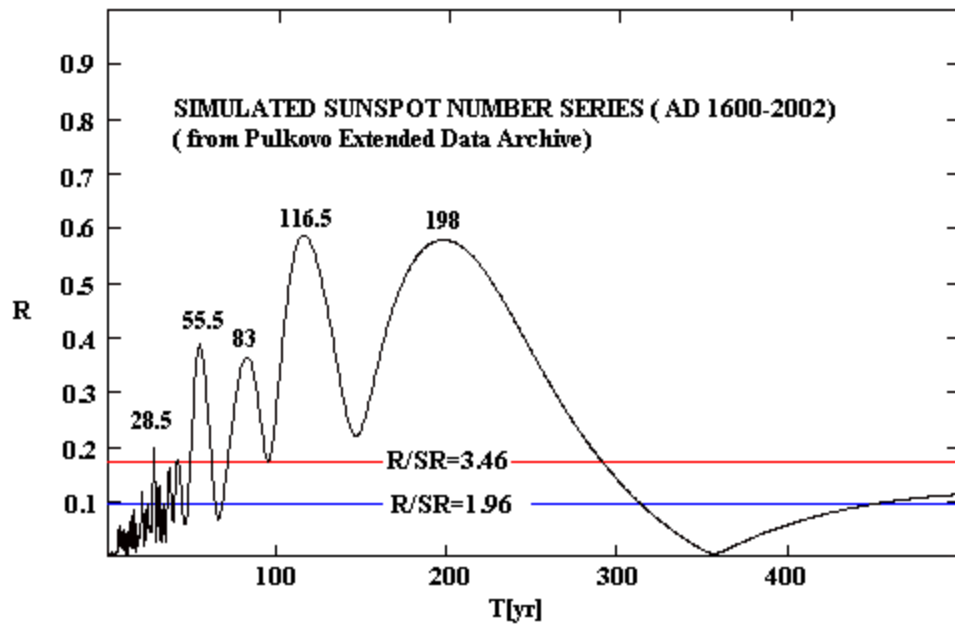


Fig. 07 T-R corellogram of the simulated sunspot *Rsi* number series (AD 1600-2002, ESAI)

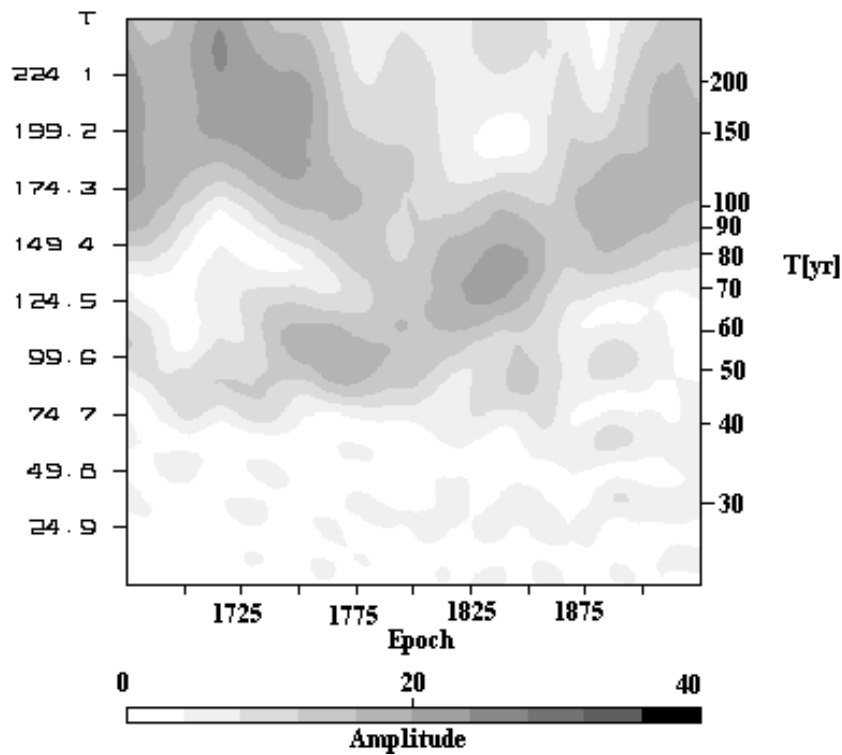


Fig. 08 The MWTRPP amplitude map of the simulated sunspot *Rsi* number series (AD 1600-2002, ESAI)

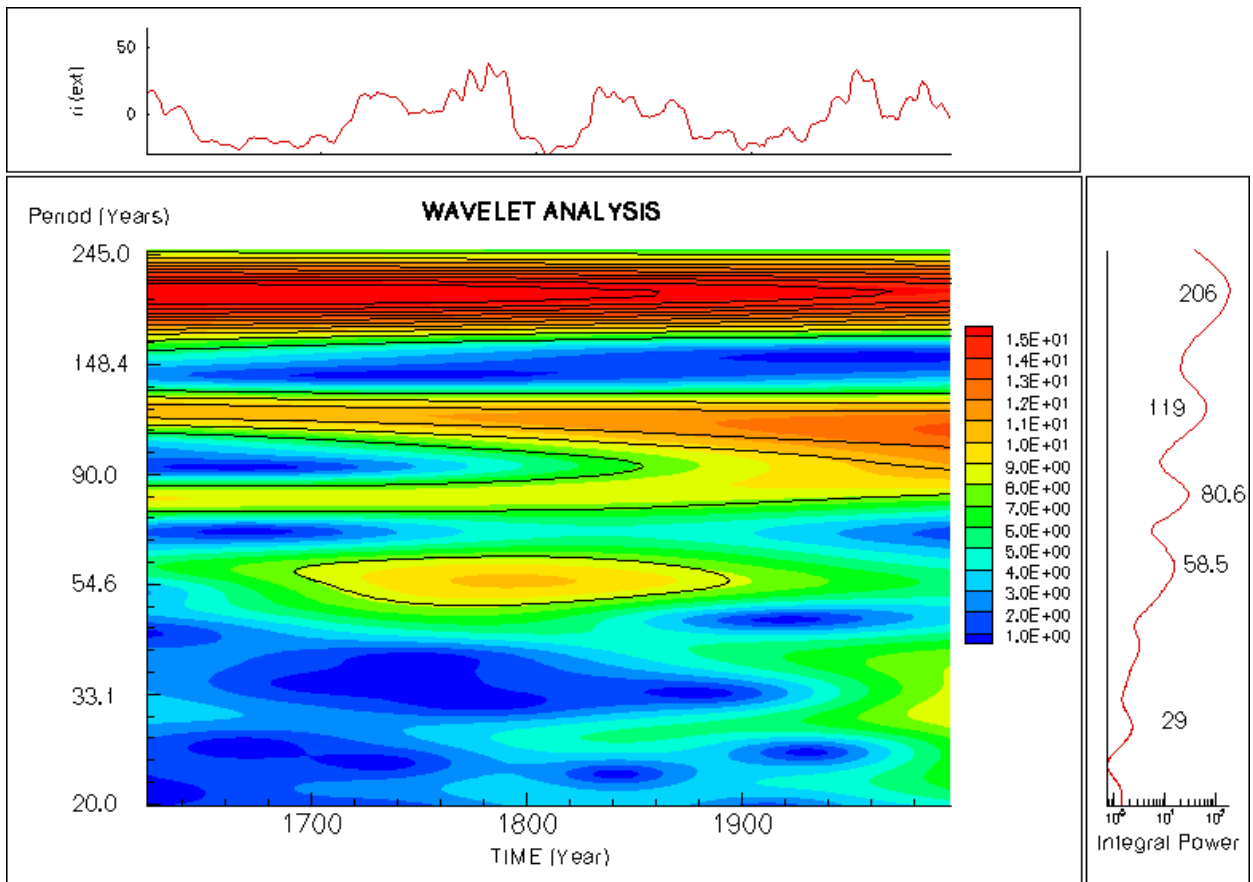


Fig. 09 WA amplitudes of the simulated sunspot R_{si} number series (AD 1600-2002, ESAI)

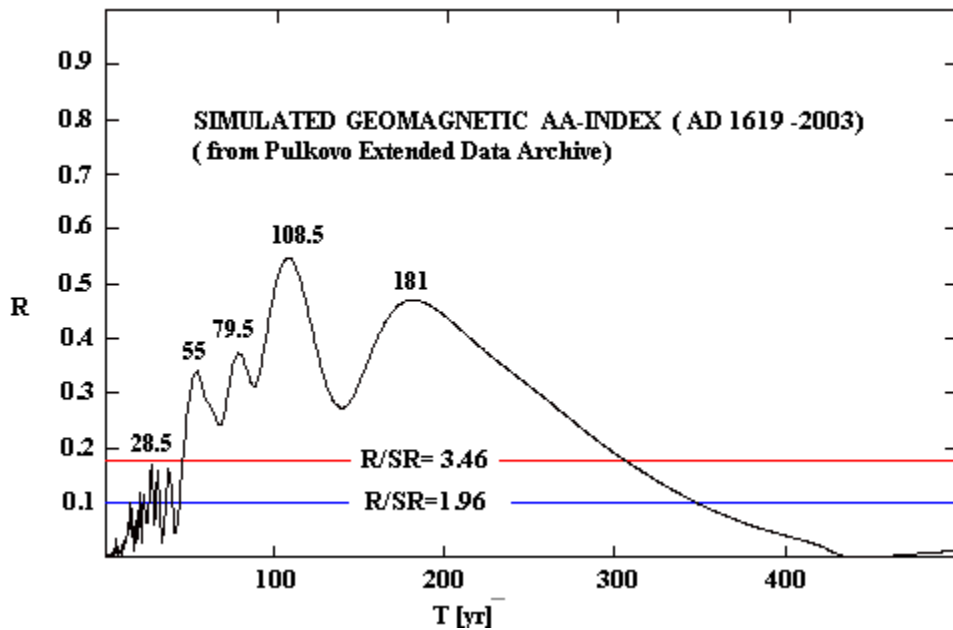


Fig. 10 T-R corellogram of the simulated aa -index (AA) data series (AD 1619-2003, ESAI):

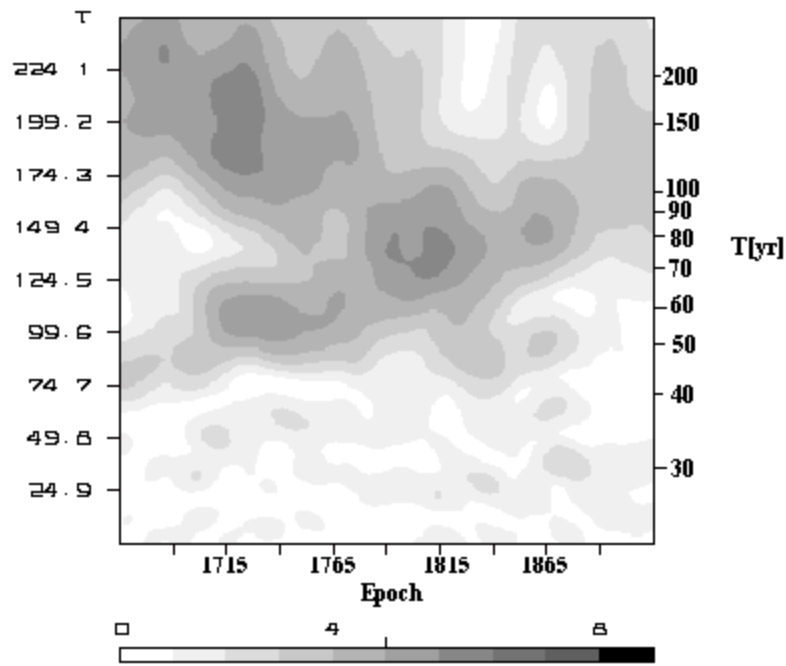


Fig. 11 The MWTRPP amplitude map of the simulated geomagnetic *aa*-index (*AA*) data series (AD 1619-2003, ESAI)

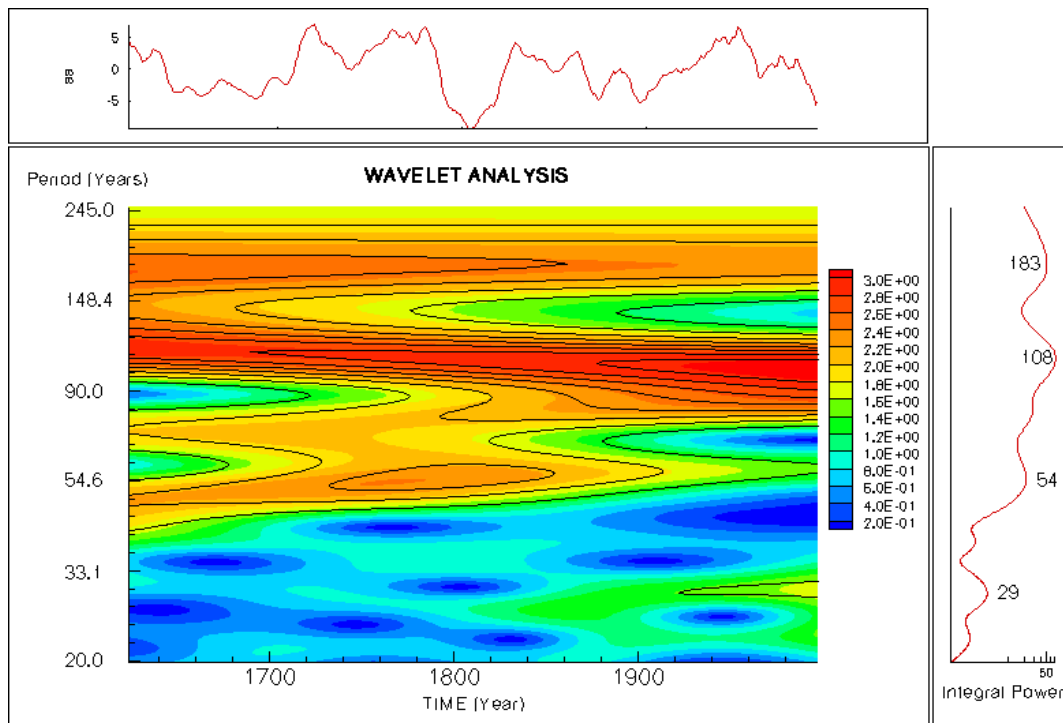


Fig. 12 WA amplitudes of the simulated geomagnetic *aa*-index (*AA*) data series (AD 1619-2003, ESAI)

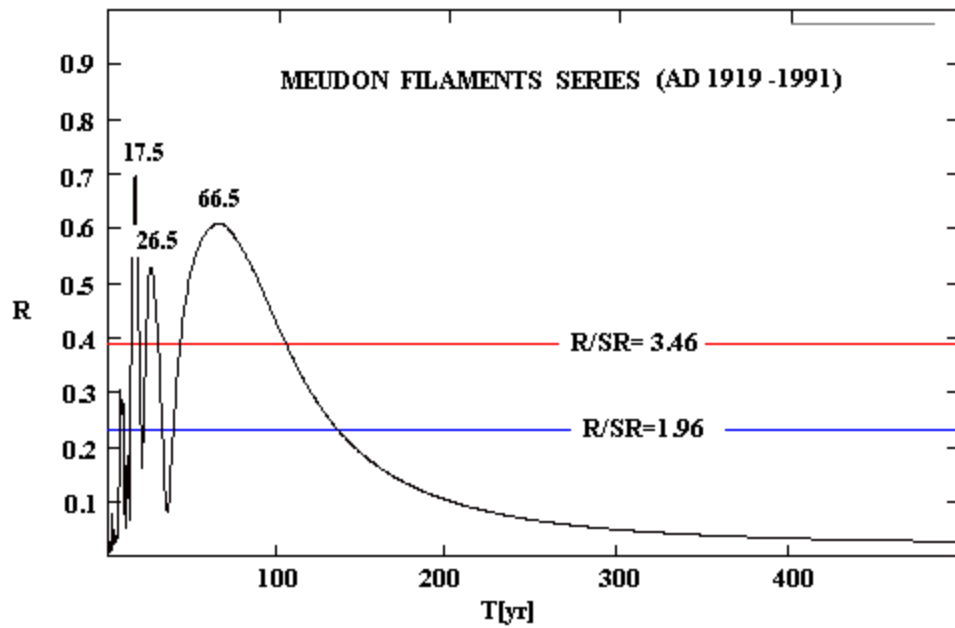


Fig 13. The T-R corellogram of the solar filaments number series from the Meudon catalogues (1919-1991)

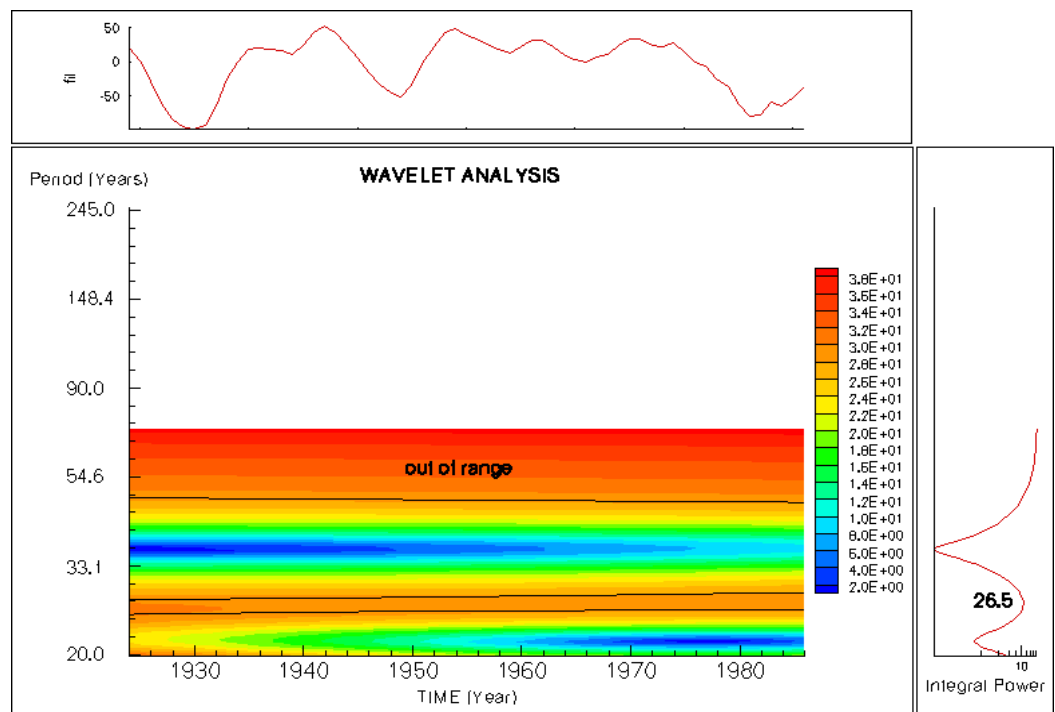


Fig. 14. Wavelet analysis of the solar filaments number series from the Meudon catalogues (1919-1991)

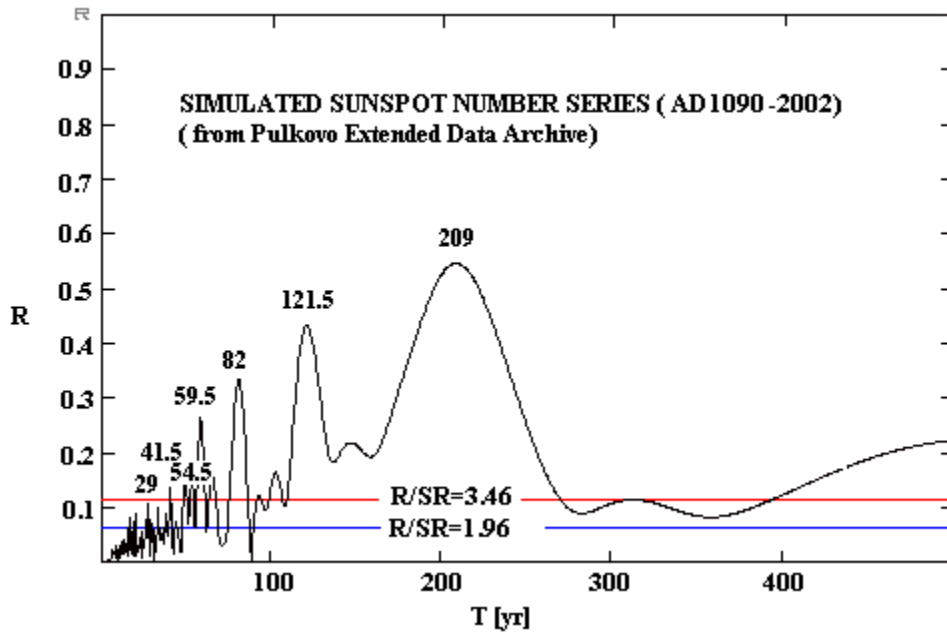


Fig. 15 T-R corellogram of the whole simulated sunspot *Rsi* number series (AD 1090-2002, ESAI)

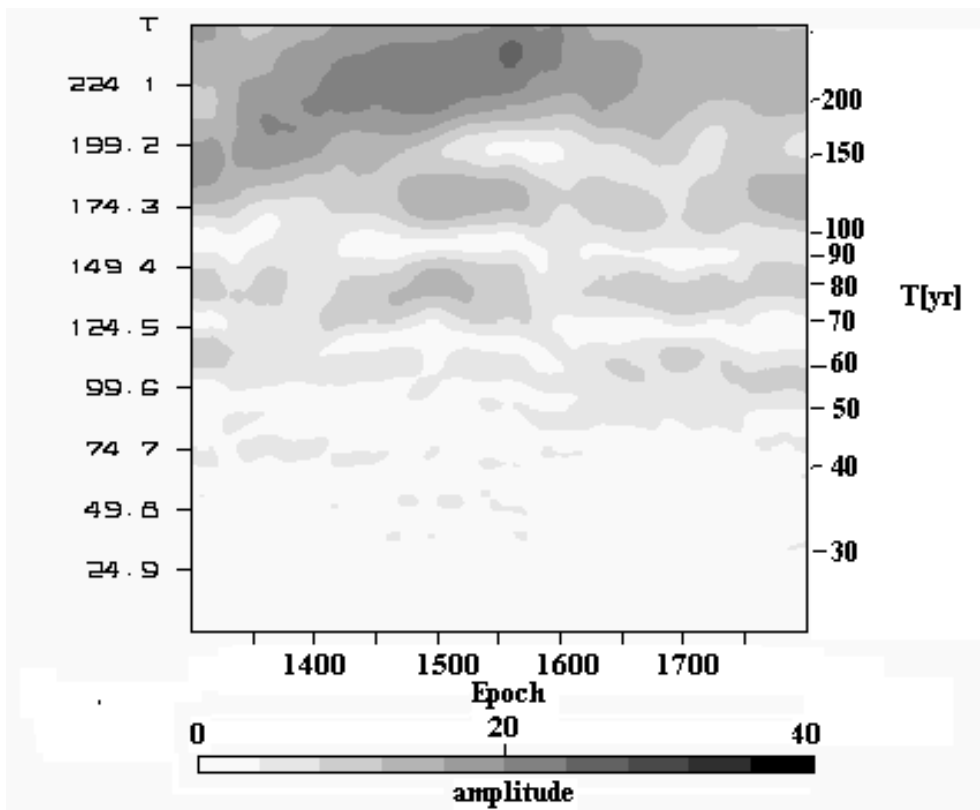


Fig. 16 The MWTRPP amplitude map of the whole simulated sunspot *Rsi* number series (AD 1090-2002, ESAI)

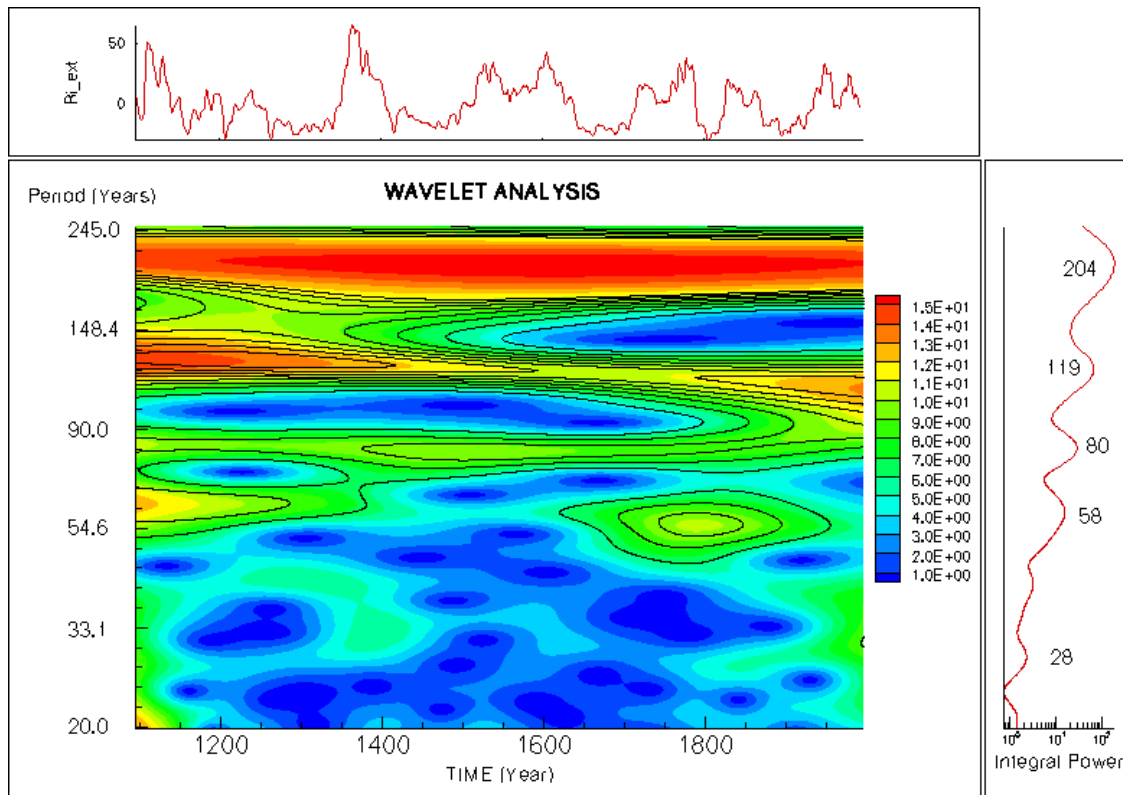


Fig. 17 WA amplitudes of the simulated geomagnetic *aa*-index (*AA*) series (AD 1099-2002, ESAI)

REFERENCES

- Ahluwalia, H.S.: 1998, *J. Geophys. Res.*, **103**, 12103.
- Ataç, T., Özgüç, A.: 1998, *Solar Phys.* **180**, 397.
- Badalyan, O.G., Obridko, V.N., Sykora, J.: 2000, *Solar Phys.* **199**, 421
- Beer, J., Blinov, B., Bonani, G., Finkel, R.C., Hofmann, H., Lelmann, B., Oeschger, H., Sigg, A., Schwander, J., Staffelbath, T., Stauffer, B., Suter, M., Gfli, W.: 1990, *Nature*, **347**, 16.
- Beer, J., Tobias, S., Weiss, N.: 1998, *Solar Phys.* **181**, 237.
- Benson, J.L., Bonev, B., James, P., Shan, K., Cantor, B., Caplinger M. : 2003, *Icarus*, **165**, 34
- Bonev, B., Penev, K., Sello, S.: 2004, *Astrophys. J.*, **605**, L81.
- Cliver, E.W.: 2006, *Adv. Space Res.* **38**, 119.
- Ciliverd, M., Clarke, E., Ulich, T., Rishbeth, H., Jarvis, M.: 2006, *Space Weather*, **4**, S09005.
- Crosby, N.B.: 2008, In Natchimuthuk Gopalswamy & David F. Webb (eds.), “*Universal Heliophysical Processes*”, IAU Symp. **257**, 47.

- Damon, P.E., Sonett, C.P.: 1991, In C. P. Sonett, M. S. Giampapa & M. S. Matthews (eds.), *The Sun in Time*, University of Arizona Press, Tucson, Arizona, 360.
- Damon, P., Peristykh, A. Meese, D.: 1997, $^{10}\text{Be/g}$: Production vs Accumulation in Recording the Schwabe and Hale Cycles, *preprint (in 18th IAGA Assembly, Aug.1997, Uppsala)*.
- Dergachev, V.A., Chistiakov, V.F.: 1993, In Yu. I. Vitinskii et al. (eds.) *Solar Cycle*, (*Leningrad: Physics-Technical Inst., Russian Acad. Sci.*), 112
- de Vries, H.: 1958, *Koninkl. Ned. Acad. Wetenschap.* **861**, 94.
- Du, Z.L.: 2006, *New Astronomy*, **12**, 29.
- Duchlev, P.: 2001, *Solar Phys.*, **199**, 211.
- Fyodorov, M.V., Klimenko, V.V., Dovgalyuk, V.V.: 1995, *Solar Phys.* **165**,193.
- Gleissberg, W.: 1944, *Terr. Magn. Atm. Electr.* **49**, 243.
- Hoyt, D.V., Schatten, K.H.: 1998, *Solar Phys.* 181, 491.
- Javaraiah, J., Bertello, L., Ulrich, R. K.: 2005, *Solar Phys.* 232, 25
- Javaraiah J., 2008, *Solar Phys.* 252, 419
- Kane, R.P.: 2008, *Ann. Geophys.* **26**, 3329.
- Kane, R.P.: 2009. *Solar Phys.* **255**, 163.
- Kiliç, H. 2009: *Solar Phys.* **255**, 155.
- Kleczek, 1952, *Bull. Astron. Inst. Czechosl.* **3**, 52.
- Kleczek, J.: 1952, *Publ. Inst. Centr. Astron.*, No. 22, Prague.
- Knoška, S., Petrásek, J.: 1984, *Contrib. Astron. Obs. Skalnaté Pleso* **12**, 165.
- Komitov, B.: 1986, *Soln. dannie*, no. 5, 73.
- Komitov, B. : 1997, *Bulg. Geoph. J.*, **23**, 74.
- Komitov, B., Bonev, B.: 2001, *Astrophys. J.* **554**, L119.
- Komitov, B., Kaftan, V.: 2003, *Geomagn. & Aeronomy*, **43**, No 5, 553.
- Komitov, B., Kaftan, V.: 2004, In A.V. Stepanov, E.E. Benevolenskaya, and A.G. Kosovichev (eds.), “*Multiwavelength analysis of solar activity*”, IAU Symp. **223**, 113.
- Komitov, B., Bonev, B., Penev, K., Sello, S.: 2004, In A. V. Stepanov, E. E. Benevolenskaya, and A. G. Kosovichev (eds.), “*Multiwavelength analysis of solar activity*”, IAU Symp. **223**, 705.
- Komitov,B.: 2007, *Bulg. Astron. J*, **9**, 107.

- Komitov, B.: 2009, *Bulg. Astron. J.*, **12**, 75.
- Komitov, B.: 2010, *Bulg. Astron. J.* **13** (in press)
- Komitov, B., Duchlev ,P., Koleva K., Dechev, M.: 2010, ArXiv: astro-ph/1007.2735
- Křivský, L., Pejml, K.: 1988, *Publ. Astron. Inst. Czech. Acad. Sci.*, No. 75.
- Lilensten, J., Bornarel, J.: 2006, *Space Weather, Environment and Societies*, Dordrecht, Springer.
- Link, F., Kleczek, J.: 1949, *Bull. Astron. Inst. Czechosl.*, **1**, 69.
- Nagovitsyn, Yu.A.: 1997, *Astron. Letters* **23**. No 6. 742.
- Nagovitsyn, Yu.A., Ivanov, V.G., Miletsky, E.V., Volobuev, D.M.: *Solar Phys.* 224, 103.
- Nagovitsyn, Yu.A.: 2006, *Astron. Letters* **32**, No 5. 382.
- Ogurtsov, M.: 2005, *Solar Phys.* **231**, 167.
- Pesnell, W.: 2009, *BAAS*, **41**, 826
- Ranucci, G., Sello, S.: 2006, *Phys. Rev. D*, **75**, 073011.
- Scargle, J.D.: 1982, *Astrophys. J.*, **263**, 835.
- Schove, D.J.: 1955, *J. Geophys. Res.*, **60**, 127.
- Schove, D.J. : 1983, *Sunspot Cycles* (Stroudsburg: Hutchinson Ross, Pennsylvania)
- Sello, S.: 2003, *New Astronomy* **8**, 105
- Solanki, S.K., Usoskin, I.G., Kromer, B., Schüssler, M., Beer, J.: 2004, *Nature*, **431**, 1084.
- Schatten, K.H., Tobiska, K.: 2003, *BAAS* **35**, 817.
- Stuiver, M., Quay, P.D.: 1980, *Science*, **207**, No 44, 26.
- Torrence, C., Compo, G.P.: 1998, *Bul. Am. Meteor. Soc.* **79**, 61.
- Usoskin, I.G., Solanki, S., Kovaltsov, G.A., Beer, J., Kromer, B.: 2006, *Geophys. Res. Let.* **33**, L08107.
- Vaquero M: 2007, [arXiv:astro-ph/0702068v1](https://arxiv.org/abs/astro-ph/0702068v1)